[17] L. Lam, R.P. Pan, M.C. Veinott, and Y.H. Chan, *Bull. Am. Phys. Soc.* **39**, 140 (1994). See also Lam [23].

[18] H. Freund and P. Grassberger, *Physica A* **190**, 218 (1992).

[19] M.M. Millonas, *J. Theor. Biol.* **159**, 529 (1992).

[20] E.M. Rauch, M.M. Millonas, and D.R. Chialvo, *Phys. Lett. A* **207**, 185 (1995).

[21] F. Schweitzer and L. Schimansky-Geier, *Physica A* **206**, 359 (1994).

[22] F. Schweitzer, K. Lau, and F. Family, Active Brownian walkers simulate trunk trail formation by ants, Preprint.

[23] L. Lam, *Chaos Solitons Fractals* **6**, 267 (1995). See also L. Lam, in *Introduction to Nonlinear Physics*, edited by L. Lam (Springer-Verlag, New York, 1996).

18
Clustering of Active Walkers: Phase Transition from Local Interactions

Frank Schweitzer and Lutz Schimansky-Geier

18.1   Introduction

The emergence of complex behavior in a system consisting of interacting simple elements is among the most fascinating phenomena of our world. Examples of these emerging new features can be found in almost every field of today's scientific interest, ranging from the behavior of social groups [1], to coherent pattern formation in physical and chemical systems [2], to the motion of swarms of animals in biology [3].

The question of how the system properties on the macroscopic level depend on the microscopic interactions is one of the major challenges in complex systems and, despite a number of different attempts [4], is far from being solved.

One of the possibilities for gaining insight into the interplay between microscopic interactions and macroscopic features in complex systems comes from computer simulations. In a very general sense, the elements or particles of the system are treated as *multiagents*, relatively autonomous entities that have a set of different rules to interact with each other. Which of the rules applies for a specific case may also depend on local variables, which in turn can be influenced by the (inter)action of the multiagents. By changing the rules of interaction or the influence of the environment during the simulation, one might be able to observe different kinds of collective behavior or even the emergence of new system properties not readily predicted from the basic equations.

Different kinds of multiagent models are applied today in the science of complex systems. Some examples are behavior-based artificial intelligence [5], artificial adaptive agents in economic theory [6], and multiagent systems in the dynamic of settlement systems [7].

One of the physical versions of the multiagent model is the active walker model, in which particles move in a space- and time-dependent potential $U(r, t)$ like an environmental potential known from theoretical ecology. The term *active* means that the particles are capable of (i) of recognizing and (ii) of altering this potential. On the other hand, a change of the potential should have a feedback on the *behavior* of the particles, for example, if it moves along a potential gradient. The active walker model has been applied to the simulation of structure formations like the dielectric breakdown in a liquid [8], the generation of rough surfaces [9], and the formation

of foraging trails of ants [10].

In the model described in this chapter, the active walkers constantly produce a chemical that locally reduces the potential and therefore attracts the walkers to the minima they just originated. It is the noise in the system that pushes them out of these minima and allows a further motion. But if the relation between the noise and the local density fluctuations of the chemical produced exceeds a critical value, a phase transition occurs that leads to the clustering of the active walkers—not by direct attachment, but by attraction to the same potential minima. This phase transition is demonstrated by computer simulations and described within an analytic approach.

18.2   Equations of Motion for the Active Walker

We consider a two-component model. The particles of the component A are the active walkers, moving on a surface characterized by a potential $U(r, t)$. The equation of motion for the N active walkers with the positions $R_1 \ldots R_N$ is given by the following Langevin equation:

$$v_i = \frac{dR_i}{dt}; \quad \frac{dv_i}{dt} = -\beta v_i - \left. \frac{\partial U(r, t)}{\partial r} \right|_{R_i} + \sqrt{2 k_B T \beta} \xi_i(t), \qquad (18.1)$$

where β is the friction coefficient of the walker ($m = 1$), $U(r, t)$ is the potential of the surface, and $\xi_i(t)$ is a white random force. As is well known, for times $t \gg t_0 = 1/\beta$ the Langevin equation can be reduced to the Einstein-Smoluchowski limit [11]

$$\frac{dR_i}{dt} = -\frac{1}{\beta} \left. \frac{\partial U(r, t)}{\partial r} \right|_{R_i} + \sqrt{\frac{2 k_B T}{\beta}} \xi_i(t). \qquad (18.2)$$

The walkers are able to interact with the surface and thus change the potential $U(r, t)$, which therefore may consist of two parts

$$U(r, t) = U_0(r, t) + U_w(r, t), \qquad (18.3)$$

where $U_0(r, t)$ means the background, which can change with time and can be influenced by external fields (like the environmental potential in ecology), and $U_w(r, t)$ is the part of the potential that is changed by the walker.

In order to specify this change, we assume that the particles of component A constantly produce a substance of component B at a rate q [$1/s$] just at the place where they are:

$$A \xrightarrow{q} A + B. \qquad (18.4)$$

If $b(r, t)$ denotes the surface density [particles/m^2] of component B, the surface potential shall be influenced by B in the following way:

$$U(r, t) = U_0 - g b(r, t). \qquad (18.5)$$

Here, the potential U_0 is set to be constant, and g means some dimensional constant [(m^2/s)^2 M/N_A], where M is the molar mass and N_A is Avogadro's number.

Inserting $U(r, t)$ in Eq. (18.5), we get the equation of motion for the single active walker as

$$\frac{dR_i}{dt} = \frac{g}{\beta} \left. \frac{\partial b(r, t)}{\partial r} \right|_{R_i} + \sqrt{\frac{2 k_B T}{\beta}} \xi_i(t). \qquad (18.6)$$

The first part of Eq. (18.6) describes the fact that the walker (component A) follows the concentration gradient of component B, whereas the second part represents the noise that keeps it moving away.

As long as the gradient of $b(r, t)$ is small and the noise is large, the walker behaves nearly as a random walker. However, for temperatures below a critical temperature, introduced in the next section, the action of the walker, which means the local production of B, can turn this Brownian motion into a locally restricted motion.

From the discrete description of the single walkers of component A we go to the space- and time-dependent walker density $a(r, t)$ by

$$\sum_{i=1}^{N} \delta(r - R_i(t)) \rightarrow N p(r, t) \rightarrow a(r, t), \qquad (18.7)$$

where $p(r, t)$ means the probability density to find a walker at the point r for a given time. Since the motion of the particles of component A obeys a Langevin equation, Eq. (18.2), for the density $a(r, t)$ the related Fokker-Planck equation holds:

$$\frac{\partial a(r, t)}{\partial t} = \frac{\partial}{\partial r} \left\{ \frac{1}{\beta} \frac{\partial U(r, t)}{\partial r} a(r, t) + D_a \frac{\partial a(r, t)}{\partial r} \right\}; \qquad D_a = \frac{k_B T}{\beta}, \qquad (18.8)$$

where D_a is the diffusion coefficient of the particles of component A. The derivative of the potential is again given by the gradient of the substance B.

$$\frac{\partial a(r, t)}{\partial t} = \frac{\partial}{\partial r} \left\{ -\frac{g}{\beta} \frac{\partial b(r, t)}{\partial r} a(r, t) + D_a \frac{\partial a(r, t)}{\partial r} \right\}. \qquad (18.9)$$

In order to specify the dynamics of component B, we consider that B, in addition to its production by the active walkers in Eq. (18.4), can independently diffuse at the surface with a diffusion coefficient D_b [m^2/s] and also decompose with time, where γ [$1/s$] is the reaction coefficient of the decomposition. That means the density of B has to obey a reaction-diffusion equation:

$$\frac{\partial b(r, t)}{\partial t} = -\gamma b(r, t) + q a(r, t) + D_b \Delta b(r, t). \qquad (18.10)$$

The active walkers prefer to turn to the local minima of $U(r, t)$, which means to the highest value of $b(r, t)$, but on the other hand, they only produce the particles of component B. Thus, we have a nonlinear feedback between the dynamics of both components A and B, and Eqs. (18.9) and (18.10) have to be solved simultaneously to find the spatiotemporal distributions for A and B.

18.3 Stability Analysis for Homogeneous Distributions

Equations (18.9) and (18.10) have a homogeneous solution, given by the average densities of component A and B:

$$a_{hom} = \langle a(r,t)\rangle = \frac{N}{S} = a_0; \qquad N = \int_S a(r,t)\,dr,$$
$$b_{hom} = \langle b(r,t)\rangle = \frac{B_{tot}}{S} = b_0; \qquad B_{tot} = \int_S b(r,t)\,dr. \tag{18.11}$$

The surface S on which the particles move is treated as a torus; that means it acts like a closed system. Therefore, diffusion cannot change the total amount B_{tot} of component B, which obeys the equation

$$\frac{dB_{tot}}{dt} = -\gamma B_{tot} + qN. \tag{18.12}$$

Assuming the initial condition $B_{tot} = 0$ for $t = 0$, the solution of Eq. (18.12) is given by

$$B_{tot}(t) = \frac{q}{\gamma}N\left(1 - e^{-\gamma t}\right) \xrightarrow{t\to\infty} \frac{q}{\gamma}N. \tag{18.13}$$

Equation (18.13) means that after an initial period, given by the time

$$t = \tau \geq 5/\gamma, \tag{18.14}$$

the total amount of component B in the system has reached more than 99% of a constant that depends on the ratio between the production and the decomposition rates, q/γ, and on the total number N of particles that produce B.

Assuming $B_{tot} = $ const, the homogeneous solution (Eq. (18.11)) for B is then given by

$$b_0 = \frac{qN}{\gamma S} = \frac{q}{\gamma}a_0. \tag{18.15}$$

Let us prove now the stability of the stationary state given by Eqs. (18.11) and (18.15). Therefore, we allow small fluctuations around a_0 and b_0:

$$a(r,t) = a_0 + \delta a \qquad \left|\frac{\delta a}{a_0}\right| \sim \left|\frac{\delta b}{b_0}\right| \ll 1. \tag{18.16}$$
$$b(r,t) = b_0 + \delta b$$

Inserting Eq. (18.16), linearization of Eqs. (18.9) and (18.10) gives

$$\frac{\partial \delta a}{\partial t} = -\frac{g}{\beta}a_0\Delta\delta b + D_a\Delta\delta a$$
$$\frac{\partial \delta b}{\partial t} = -\gamma\delta b + q\delta a + D_b\Delta\delta b. \tag{18.17}$$

With

$$\delta a \sim \delta b \sim \exp\{\lambda t + i k\vec{r}\}, \tag{18.18}$$

the dispersion relation for small inhomogeneous fluctuations with wave numbers results:

$$\lambda_{1,2} = -\frac{1}{2}\{\gamma + k^2(D_a + D_b)\}$$

$$\pm \sqrt{\frac{1}{4}\{\gamma + \vec{k}^2(D_a + D_b)\}^2 - \vec{k}^2 D_a(\gamma + \vec{k}^2 D_b) + \vec{k}^2\frac{g}{\beta}qa_0}. \tag{18.19}$$

For homogeneous fluctuations ($\vec{k} = 0$), we obtain

$$\lambda_1 = -\gamma; \qquad \lambda_2 = 0 \qquad \text{for} \quad \vec{k} = 0, \tag{18.20}$$

expressing the conservation of the total number of active walkers and the stability of the field $b(r,t)$ for this case. On the other hand, the system is stable against inhomogeneous fluctuations ($\vec{k} \neq 0$) as long as the relation holds:

$$D_a > D_a^{crit}; \quad \text{with} \quad D_a = \frac{k_B T}{\beta} \quad \text{and} \quad D_a^{crit} = \frac{1}{\beta}\left(\frac{gqa_0}{\gamma + D_b\vec{k}^2}\right). \tag{18.21}$$

Equation (18.21) determines a critical diffusion coefficient of component A, below which inhomogeneous fluctuations of a certain size may result in a self-collapsing behavior of the system for a given temperature. From the limit $\vec{k} \to 0$, we can obtain a critical temperature T_c from Eq. (18.21), where for $T > T_c$ the system remains stable even against large fluctuations:

$$T_c = \frac{g}{k_B}\frac{qN}{\gamma S}. \tag{18.22}$$

Introducing the parameter $\eta = T/T_c$, which refers to the thermal noise, we can rewrite the stability condition in Eq. (18.21) to obtain a relation between the thermal noise and the density fluctuations of wave number $\vec{k}$:

$$\eta = \frac{T}{T_c} > \frac{1}{1 + \frac{D_b}{\gamma}\vec{k}^2}. \tag{18.23}$$

Fluctuations below a critical wave number $\vec{k}$ determined by Eq. (18.23) result in the establishment of inhomogeneities in the distributions $a(r,t)$ and $b(r,t)$ and lead to a phase transition (Fig. 18.1).

18.4 Estimation of an Effective Diffusion Coefficient

Let us now discuss the case for which $b(r,t)$ relaxes faster, compared to $a(r,t)$, into its stationary state and the diffusion coefficient D_b is very small. This means that, depending on the thermal noise, the system is even more unstable against fluctuations, as indicated by Eq. (18.23). From the quasistationary assumption for component B, we get

$$\frac{\partial b(r,t)}{\partial t} \approx 0 \quad \rightarrow \quad b(r,t) = \frac{q}{\gamma}a(r,t); \quad \text{if} \quad D_b \to 0. \tag{18.24}$$
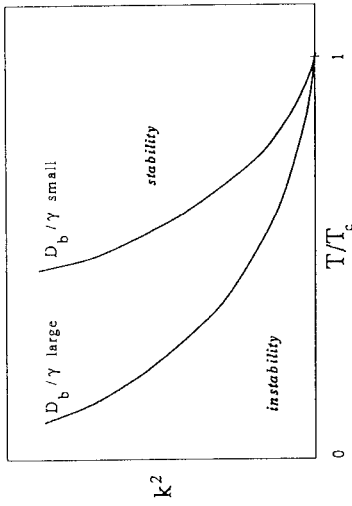
FIGURE 18.1. Instability region of the homogeneous system for density fluctuations of wave number k dependent on the temperature T (Eq. (18.23)).

The Fokker-Planck equation, Eq. (18.9), for the particle density $a(r,t)$ can be rewritten in terms of a usual diffusion equation by introducing an effective diffusion coefficient D_a^{eff}:

$$\frac{\partial a(r,t)}{\partial t} = \frac{\partial}{\partial r}\left\{ D_a^{eff}\frac{\partial a(r,t)}{\partial r}\right\}; \quad D_a^{eff} = D_a - \frac{g}{\beta}\frac{\partial b(r,t)}{\partial a(r,t)}, \quad (18.25)$$

where D_a^{eff} depends on the distribution of the active walkers, $a(r,t)$, and on the relation between the densities $b(r,t)$ and $a(r,t)$. In the quasistationary limit of Eq. (18.24), the effective diffusion coefficient for the particles of component A in Eq. (18.25) reads

$$D_a^{eff} = D_a - \frac{g}{\beta}\frac{q}{\gamma}a(r,t) = \frac{1}{\beta}\{k_BT - gb(r,t)\}. \quad (18.26)$$

We notice that the effective diffusion coefficient is not necessarily always larger than zero, which means a spreading of particles over the whole surface. It can also be less than zero, resulting in a lump of particles that keep themselves only in a certain region on the surface—what we now call a cluster. This transition is driven by the local chemical production of the active walkers. If the density $b(r,t)$ locally exceeds a certain equilibrium value, D_a^{eff} becomes negative. The phase separation line, defined by $D_a^{eff} = 0$, determines this equilibrium density $b_{eq}(T)$, which depends only on temperature:

$$D_a^{eff} = 0; \quad b_{eq}(T) = \frac{k_BT}{g}. \quad (18.27)$$

The ratio

$$\varepsilon(r,t,T) = \frac{D_a^{eff}}{D_a} = 1 - \frac{b(r,t)}{b_{eq}(T)}, \quad (18.28)$$

where $b(r,t)/b_{eq}(T) > 1$ defines the local supersaturation. In order to determine the equilibrium value $b_{eq}(T)$, we consider the critical temperature T_c of the system, where D_a^{eff} has to be always positive, because no agglomeration occurs for $T > T_c$. Inserting the expression for T_c in Eq. (18.22) into Eq. (18.27), we get $b_{eq}(T_c)$:

$$b_{eq}(T_c) = \frac{k_BT_c}{g} = \frac{B_{tot}}{S} = \frac{qN}{\gamma S}, \quad (18.29)$$

which concurs with the mean density of component B. This leads to the expression for the equilibrium concentration,

$$b_{eq}(T) = \frac{qN}{\gamma S}\frac{T}{T_c} = \frac{qN}{\gamma S}\eta, \quad (18.30)$$

and we get finally the effective diffusion coefficient $\varepsilon(r,t,T)$, Eq. (18.28) which depends on the thermal noise:

$$\varepsilon(r,t,\eta) = 1 - \frac{b(r,t)}{\eta}\frac{\gamma S}{qN}. \quad (18.31)$$

18.5 Results of Computer Simulations

Generally, the simulated behavior of an active walker obeys the following schedule:

1. The walker checks the local potential $U(r,t)$.

2. Depending on the value of $U(r,t)$, the walker makes a decision for the next step. (a) Deterministic active walker: It always follows this decision. (b) Probabilistic active walker: Because of the influence of noise, it follows this decision only with a certain probability.

3. The walker changes the local potential depending on a special rule to be determined.

4. The walker moves (stepwise). → repeat 1.

In the considered case, the local potential is given by the density of component B. Since B is produced by A, the condition at $t = 0$ is

$$U(r,0) = U_0 = const; \quad b(r,0) = 0 \quad \text{for all } r \in S. \quad (18.32)$$

The N active walkers are initially randomly distributed on the surface. Their motion is simulated on a two-dimensional hexagonal lattice with periodic boundary conditions. Since the walker makes its decision for the next step before changing the local potential, the motions of the walkers are updated sequentially, and it is also allowed that a site is occupied by more than one walker.

The walker is able to recognize the potential of its six nearest neighbor sites and to compare it with the potential value on its site, which means it measures the local

potential gradient. It then makes its decision for the next step as a probabilistic walker, which means, because of the noise, the walker sometimes ignores the attraction of the potential and finds itself out of the potential minima.

The density profile of component B (which is the inverse of the potential), which results from diffusion, decomposition, and the interaction between the components A and B in Eq. (18.10), is presented in the time series of Figs. 18.2 and 18.3. For the decomposition rate, $\gamma = 0.001$, used during the simulation, we can conclude from Eq. (18.14), that at $t = 5000$ time steps the production of B has reached its stationary value, leading to a competitive regime for the further dynamics. Figure 18.2 presents the evolution of the density $b(r, t)$ during the regime of independent growth. The random density spots, produced by the 100 active walkers in the very beginning (Fig. 18.2a), evolve into a very jagged surface profile characterized by a reduced number of peaks of comparable height (Fig. 18.2c) at about $t = 1000$.

The same picture is seen in Fig. 18.3a on a scale reduced by 10. Figure 18.3b gives the density distribution at the beginning of the competition process, which relaxes after a long time into a one-peak distribution, as already indicated in Fig. 18.3d. The selection among the different density spikes [12] can be well described in terms of a selection equation of the Eigen-Fisher type [13].

Figure 18.4 shows the spatiotemporal distribution of the effective diffusion coefficient in Eq. (18.31) during the competition regime. The inhomogeneously distributed black areas indicate a negative effective diffusion coefficient, resulting in an agglomeration of the active walkers in that area. As shown, the attraction area decreases with time in diversity as well as in area, indicating again the selection process among the attraction areas and the clustering of the walkers.

18.6   Conclusions

We have discussed a two-component reaction–diffusion system. The particles of component A are *active* in the sense that they are able (i) to recognize and (ii) to change the local potential, which determines their further motion. This nonlinear feedback is simulated by a chemical reaction of A, describing the production of a second component B, which decreases the potential locally. B can also decompose and diffuse.

We have shown that a homogeneous distribution of both components is unstable against fluctuations of a certain wave number, resulting in evolving inhomogeneities. This phase transition is driven by the local chemical production of the active walkers. We found an equilibrium density $b_{eq}(T)$ for the chemical produced. If the walkers increase the local density $b(r, t)$ above the equilibrium value, the system turns locally into a supersaturated state, which leads to the clustering of the walkers. This can be expressed by an effective diffusion coefficient D_a^{eff}, which becomes negative in this case, meaning that the spreading of the walkers over the whole system is locally turned into an attraction. Depending on the spatiotemporal density distribution $b(r, t)$, at the same time D_a^{eff} can have quite the opposite effect at different places.
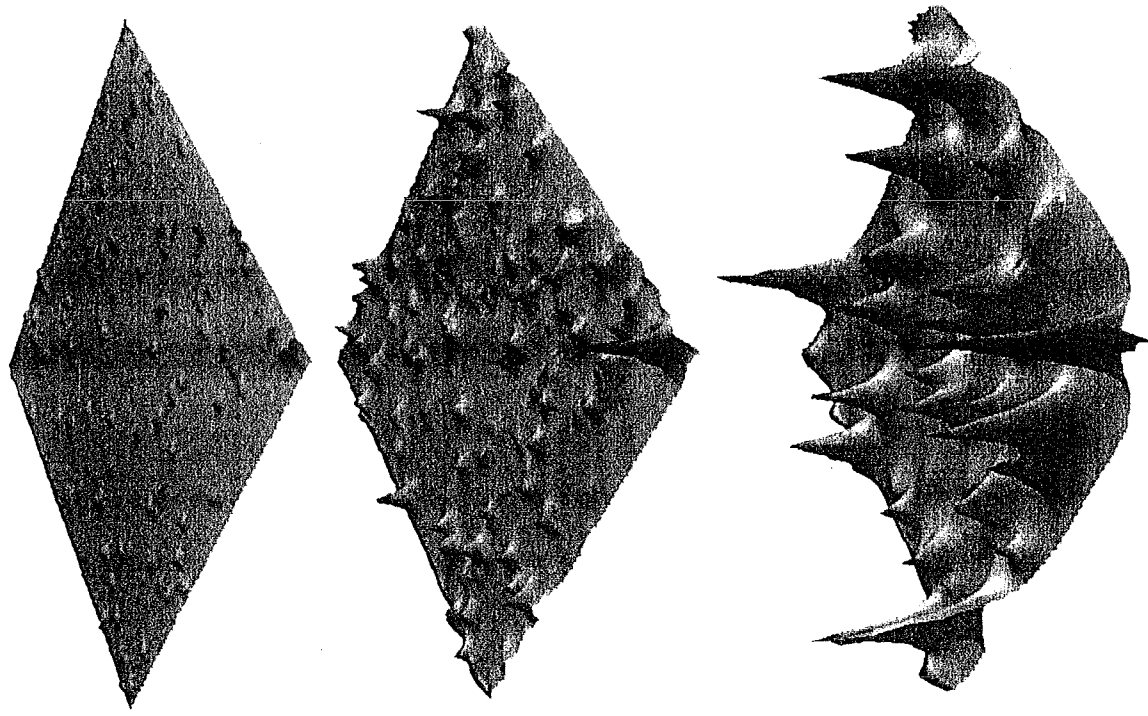

FIGURE 18.2. Evolution of the particle density $b(r, t)$ (Eq. (18.10)) during the growth regime time in simulation steps: (a) $t = 10$, (b) $t = 100$, (c) $t = 1.000$; parameters: N = 100, S = 100 × 100, T = 0.4 T_c ($\eta = 0.4$), $q = 80$, $\gamma = 0.001$, $D_b = 0.01$.
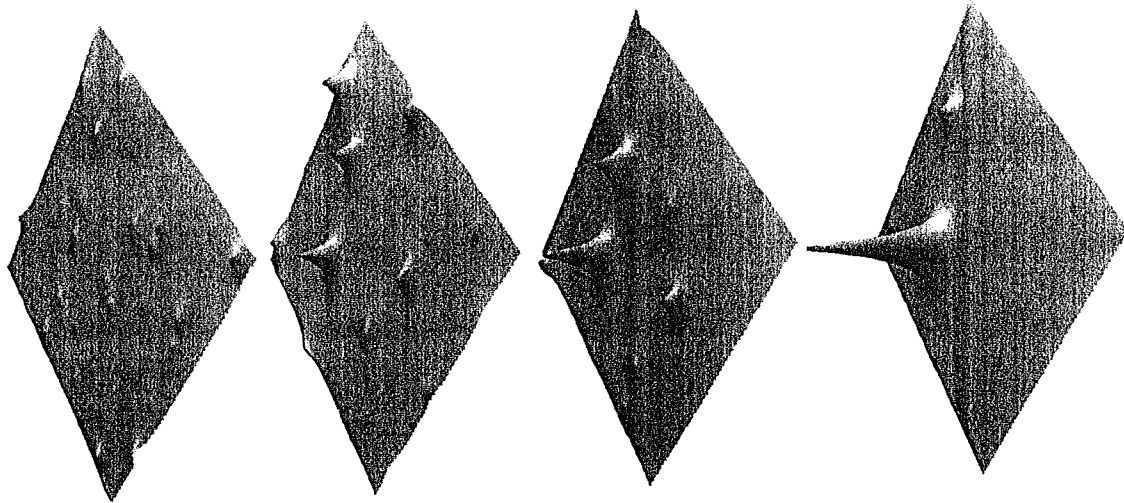
FIGURE 18.3. Evolution of the particle density $b(r, t)$ (Eq. (18.10)) during the competition regime time in simulation steps: (a) $t = 1.000$, (b) $t = 5.000$, (c) $t = 10.000$, (d) $t = 50.000$. The density scale is 0.1 times the scale of Fig. 18.2. Figure 18.3a is the same as Fig. 18.2c and illustrates the differences of the scales; parameters: see Fig. 18.2.
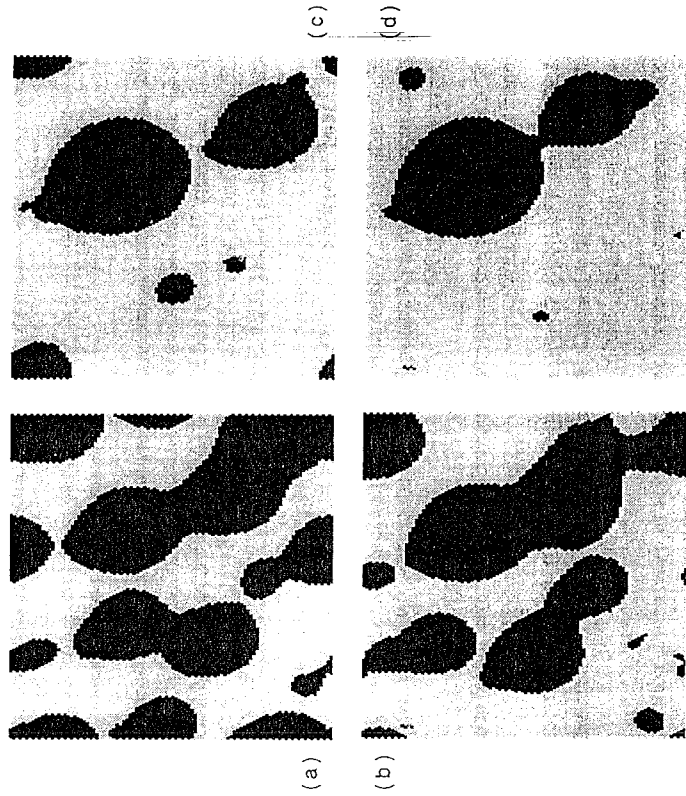
FIGURE 18.4. Spatiotemporal evolution of the effective diffusion coefficient $\varepsilon(r, t, \eta)$ (Eq. (18.31)) during the simulation of Fig. 18.3 (competition regime). The black area indicates $\varepsilon < 0$, which means an attraction area for the active walkers. The grey area indicates $\varepsilon > 0$. Time in simulation steps: (a) $t = 5.000$, (b) $t = 10.000$, (c) $t = 25.000$, (d) $t = 50.000$. Parameters: see Fig. 18.2.

Since the production of B reaches a stationary value, we found a two-step scenario for the evolution of the system: an earlier stage of independent production of B and a late stage of competition among the B-rich areas, finally leading to a one-peak distribution.

We want to point out that the basic features discussed within this chapter, have a range of analogies within biological systems, for example, to the chemotaxis of ants, which lay a pheromone into the ground [14] to use it for their orientation or, in general, to stigmergic processes [15], which are important in swarm behavior.

What is it about the active role that noise plays in this system? Based on nonlinear feedback, the particles are forced to increase an initial concentration fluctuation, which in turn prevents their further movement. Noise plays an important role in the

sense that it allows the particles to keep moving as long as the density fluctuations are small enough; it is therefore crucial for the establishment of the large density spikes that finally mark the phase transition.

18.7   Acknowledgments

18.8   References

[1] E. Jantsch and C.H. Waddington, eds., *Evolution and Consciousness. Human Systems in Transition* (Addison-Wesley, Reading, MA, 1976); W. Weidlich, *Phys. Rep.* **204**, 1 (1991).

[2] S. Kai, ed., *Pattern Formation in Complex Dissipative Systems* (World Scientific, Singapore, 1992).

[3] E.O. Wilson, *The Insect Societies* (Belknap, 1971); B. Pfistner, in *Biological Motion*, edited by W. Alt and G. Hoffmann, *Lecture Notes in Biomathematics*, vol. 89, (Springer-Verlag, Berlin, 1990), pp. 556–565.

[4] See the numerous volumes of *Springer Series in Synergetics*, edited by H. Haken (Springer-Verlag, Berlin) or *Santa Fe Institute Studies in the Sciences of Complexity* (Addison-Wesley, Reading, MA).

[5] D. Jefferson, R. Collins, C. Cooper, M. Dyer, M. Flowers, R. Korf, C. Taylor, and A. Wang, in *Artificial Life II*, edited by C. Langton, C. Taylor, J. Doyne Farmer, and S. Rasmussen (Addison-Wesley, Reading, MA, 1992), pp. 549–578.

[6] J.H. Holland and J.H. Miller, *AEA Papers Proc.* **81**(2), 365 (1991).

[7] S. Bura, F. Guerin-Pace, H. Mathian, D. Pumain, and L. Sanders, preprint (P.A.R.I.S.), 1994.

[8] D. R. Kayser, L.K. Aberle, R.D. Pochy, and L. Lam, *Physica A* **191**, 17 (1992).

[9] L. Lam, R.D. Freimuth, M.K. Pon, D.R. Kayser, J.T. Fredrick, and R.D. Pochy, in *Pattern Formation in Complex Dissipative Systems*, edited by S. Kai (World Scientific, Singapore, 1992), pp. 34–46.

[10] F. Schweitzer, K. Lao, and F. Family (submitted for publication).

[11] L. H'walisz, P. Jung, P. Hänggi, P. Talkner, and L. Schimansky-Geier, Z. *Phys. B* **77**, 471 (1989).

[12] F. Schweitzer and L. Schimansky-Geier, *Physica A* **206**, 359 (1994).

[13] W. Ebeling and R. Feistel, *Physik der Selbstorganisation und Evolution* (Akademie-Verlag, Berlin, 1986).

[14] V. Calenbuhr and J.-L. Deneubourg, in *Biological Motion*, edited by W. Alt and G. Hoffmann, *Lecture Notes in Biomathematics*, vol. 89 (Springer-Verlag, Berlin, 1990), pp. 453–469.

[15] M. Millonas, *J. Theor. Biol.* **159**, 529 (1992).